Production potential of seaweed and shellfish integrated aquaculture in Narragansett Bay (Rhode Island, U.S.) using an ecosystem model

Romain Lavaud [a], David S. Ullman [b], Celeste Venolia [c], Carol Thornber [d], Lindsay Green-Gavrielidis [e], Austin Humphries [b,c,*]

[a] *School of Renewable Natural Resources, Louisiana State University Agricultural Center, Baton Rouge, LA, United States*
[b] *Graduate School of Oceanography, University of Rhode Island, Narragansett, RI, United States*
[c] *Department of Fisheries, Animal and Veterinary Sciences, University of Rhode Island, Kingston, RI, United States*
[d] *Department of Natural Resources Science, University of Rhode Island, Kingston, RI, United States*
[e] *Department of Biology and Biomedical Sciences, Salve Regina University, Newport, RI, United States*

A B S T R A C T

Integrated aquaculture systems combining macroalgae with traditional fish and shellfish production represent an ecologically sound and economically attractive solution for farmers. To evaluate the potential of growing sugar kelp (*Saccharina latissima*) at existing oyster (*Crassostrea virginica*) farms in Narragansett Bay (NB; Rhode Island, U.S.), we developed an ecosystem model based on individual Dynamic Energy Budget models for kelp and oysters forced offline by a coupled 3D hydrodynamic-water quality model. Kelp growth during the cold winter months provides ecosystem services through the removal of nutrients in the bay as well as serving as an additional source of revenue for farmers. Locations with the most nutrient-rich waters at the northern end of the bay seem most suitable for kelp aquaculture, with oyster growth also reaching maxima at the same locations. Predictions of kelp biomass grown on lines ranged from 0.97 kg_{WW} m^{-1} at the easternmost site at the Bay Entrance to 2.03 kg_{WW} m^{-1} at the northernmost site in the Upper Bay, or 1.6 and 3.4 tons ha^{-1} on 6 m spaced line-farms, respectively. For denser production in 1.5 m spaced line-farms, estimates ranged between 6.5 and 13.5 tons ha^{-1}. Depending on the different farm setups, we estimated the potential profits (based on delivered cost for consumer product) at $4,468 for a 6 m spaced line-farm of 1 ha and $17,872 for a 1.5 m spaced line-farm. The N and C fixation of kelp ranged depending on spacing of longlines and time of harvest but reached maximum values of 1117 and 6184 kg ha^{-1}, respectively. These estimates offer valuable information that should help producers and managers in their decision to direct efforts and investments into this developing activity in the U.S.

1. Introduction

Estuarine and coastal ecosystems provide essential goods and services including provision of fisheries, foraging and nursery habitat, filtration, and detoxification (Barbier et al., 2011). However, they are also increasingly affected by anthropogenic activities through eutrophication, overfishing, pollution, and habitat degradation (Lotze et al., 2006; Worm et al., 2006; Barbier et al., 2011). This has led to increasing investments in coastal restoration as well as motivating coastal communities to search for alternative solutions to sustain livelihoods. In this context, aquaculture has become the fastest growing form of aquatic food production and now represents more than half of all seafood production globally (FAO, 2020). Unfortunately, the rapid development of

aquaculture has led to some negative social-ecological impacts, particularly from large-scale fish farms (Bostock et al., 2010). Culture of lower trophic level species are generally far less damaging to the environment and can even improve the health of ecosystems (Gallardi, 2014). Although great efforts have been undertaken to mitigate the negative impacts from aquaculture, different approaches are needed that deliver aquatic food within ecological limits while conserving and/or restoring ecosystem goods and services.

Integrated aquaculture, i.e., raising multiple species of different trophic levels to recreate natural ecosystem dynamics, has been practiced by many societies throughout history. Shellfish and seaweeds provide a range of valuable ecosystem goods and services (Cabral et al., 2016; Smaal et al., 2019) and similar functions can be ascribed to their

commercial cultivation. Those functions include provision of food (Grant and Strand, 2019; FAO 2020), wildlife habitat for fish and mobile invertebrate species (Tallman and Forrester, 2007; Theuerkauf et al., 2021), water quality regulation (Chopin et al., 1999; Gallardi, 2014; Smaal et al., 2019), coastal protection (Jackson and Winant, 1983; Ysebaert et al., 2019), and carbon sequestration (Tang et al., 2011). In the last decade, an increasing body of literature has highlighted and promoted these approaches to offer solutions that ensure sustainable ecological, social, and economic objectives (e.g., Chopin et al., 1999; Holdt and Edwards, 2014). As a result, shellfish and seaweed aquaculture is increasingly considered as a solution to mitigate negative anthropogenic impacts in aquatic environments while also providing a wide array of ecosystem goods and services (European Commission, 2012; Froehlich et al., 2017).

While the U.S. ranks among the world leaders in fisheries production, aquaculture remains a modest industry with little growth. Shellfish production has been at a relatively constant level since 2014, although it still leads U.S. aquaculture production in value (NMFS, 2021). Most of the growth in U.S. aquaculture comes from new seaweed cultivation, especially in New England (Kim et al., 2019) and Alaska (NOAA Alaska Fisheries Science Center, 2022). Seaweed aquaculture can maintain its momentum by emphasizing its environmental benefits, the diversification of its products, and the cultivation of a variety of native species. Moreover, the combination of shellfish with seaweed aquaculture could also be a diversification opportunity for shellfish farmers towards economic stability in an industry where success is deeply conditioned by the increasing variability of environmental factors and markets (Smith, 2019; Stankus, 2021). However, complex permitting processes and social resistance to aquaculture are often cited as barriers to expansion (Knapp and Rubino, 2016). For example, empirical research from Rhode Island shows that public support for farms is positively associated with societal impacts rather than those associated with environmental impacts (Dalton and Jin, 2018). Another impediment to aquaculture growth is uncertainty surrounding the growth potential of organisms, which affects the economic potential of farms (Gibbs, 2009). Little is known regarding suitable conditions for seaweed and shellfish integrated aquaculture in the U.S., and spatially explicit estimates are needed to assist in site selection. A better understanding of the production potential of the surrounding ecosystem could help managers and farmers choose the right kind of aquaculture to grow a marketable product, while also decreasing potential negative environmental impacts and maximizing ecosystem services.

Ecosystem modeling is an important tool for aquaculture that can generate valuable information for planning and predicting ecological and economic suitability (Ferreira et al., 2007). Scenario building allows the exploration of management strategies and environmental risks to both the farming industry and the natural environment where it is implemented. Most ecosystem models integrate time and space to understand complex physical, chemical, and ecological dynamics, particularly in coastal areas where most shellfish and seaweed aquaculture facilities are located (e.g., Dowd, 2005; Cranford et al., 2013). The complexity of coastal ecosystems imposes a common trade-off between the generality and replicability (or simplicity) of a model and its realism (or precision; Matthewson and Weisberg, 2009; Kellner et al., 2011). One modeling approach often used is individual-based modeling, in which the growth of an organism (finfish, shellfish, or seaweed) is predicted based on experienced environmental conditions. Combined with a detailed formulation of physical variables (to ensure realism) and a mechanistic implementation of individual bioenergetics (to ensure generality; Guyondet et al., 2015; Lavaud et al., 2020), this approach allows for a quantitative assessment of temporal dynamics, which is needed to evaluate the benefits of integrated aquaculture (Barrett et al., 2022).

In this study, we build an ecosystem model to investigate the production potential and spatial variability of kelp and oyster growth in integrated aquaculture settings across the Narragansett Bay ecosystem (Rhode Island, U.S.). Existing models for the individual bioenergetics of sugar kelp (*Saccharina latissima*) and eastern oyster (*Crassostrea virginica*) were combined with a coupled hydrodynamics-water quality model to evaluate the influence of biogeophysical processes on the growth potential of kelp and oysters at existing shellfish leases in Narragansett Bay. Specifically, we used model simulations to identify optimal geographic locations and harvest timing for kelp farming. This ecosystem model provides new estimates of kelp and oyster growth potential that should help inform farmers and local managers in their decision to adopt integrated kelp and oyster aquaculture in Rhode Island and elsewhere where their growth is feasible.

2. Material and methods

2.1. Study site

The ecosystem model presented in this study was developed for Narragansett Bay (NB), a 381 km^2 estuarine system along the Northeast coast of the U.S (Fig. 1a) where oyster farming is well developed. Most of the farming is conducted using on-bottom rack and bag systems, but this can be variable and include floating bags. For this study, we only focus on on-bottom culture and divide the oyster farm sites in NB into several sub-areas that roughly correspond with the local geography, and which lie along the dominant north-south hydrographic gradient (Fig. 1b). From north to south, the salinity generally increases from the Upper Bay through the Mid and Lower Bay sub-areas and is highest at the Bay Entrance sites. Nutrient concentrations (e.g. nitrate) exhibit a reversed gradient, with highest values in the Upper Bay and lowest values in the Bay Entrance sub-area. The Sakonnet sub-area in the easternmost portion of NB is somewhat isolated geographically from the rest of the Bay by the narrow entrance at its northern end but is significantly influenced by freshwater discharge from the Taunton River (the easternmost river entering NB shown in Fig. 1a). Hydrographically, the Sakonnet sub-area is like the Mid Bay sub-area. The oyster farm sites in the Sakonnet sub-area are somewhat shallower than elsewhere in the Bay.

2.2. Ecosystem model

The ecosystem model is composed of three models: a coupled hydrodynamics-water quality model (OSOM-CoSiNE) and two individual bioenergetic (Dynamic Energy Budget; DEB) models, one for kelp and one for oysters (Fig. 2). The OSOM-CoSiNE model consists of a 3D hydrodynamics module simulating the circulation and hydrography (temperature and salinity), and a biogeochemical module computing the lower trophic level ecology of NB to provide concentrations of dissolved inorganic carbon (DIC), dissolved inorganic nitrogen (DIN), and plankton. Photosynthetically active radiation (PAR) was derived from radiative forcing from the North American Regional Reanalysis (Venolia et al., 2020). Temperature, PAR, and nutrient concentrations were used as forcing variables for the kelp model to predict blade growth (blade length; cm). Temperature and plankton concentration were used as forcing variables for the oyster model to predict shell (and tissue) growth (shell height; cm).

2.3. Hydrodynamics-water quality model

The three-dimensional hydrodynamics of NB were computed using the Ocean State Ocean Model (OSOM; Sane et al., 2020), which is an application of the Regional Ocean Modeling System (ROMS; Shchepetkin and McWilliams, 2005). The model domain extends from the upper reaches of NB to the mid-shelf off the southern New England coast (Fig. 1a). The spatial grid consists of 1000 × 1100 cells with a curvilinear varying horizontal resolution of approximately 85 m near the head of NB and 475 m at the southern boundary. There are 15 terrain-following vertical levels. Other model properties including
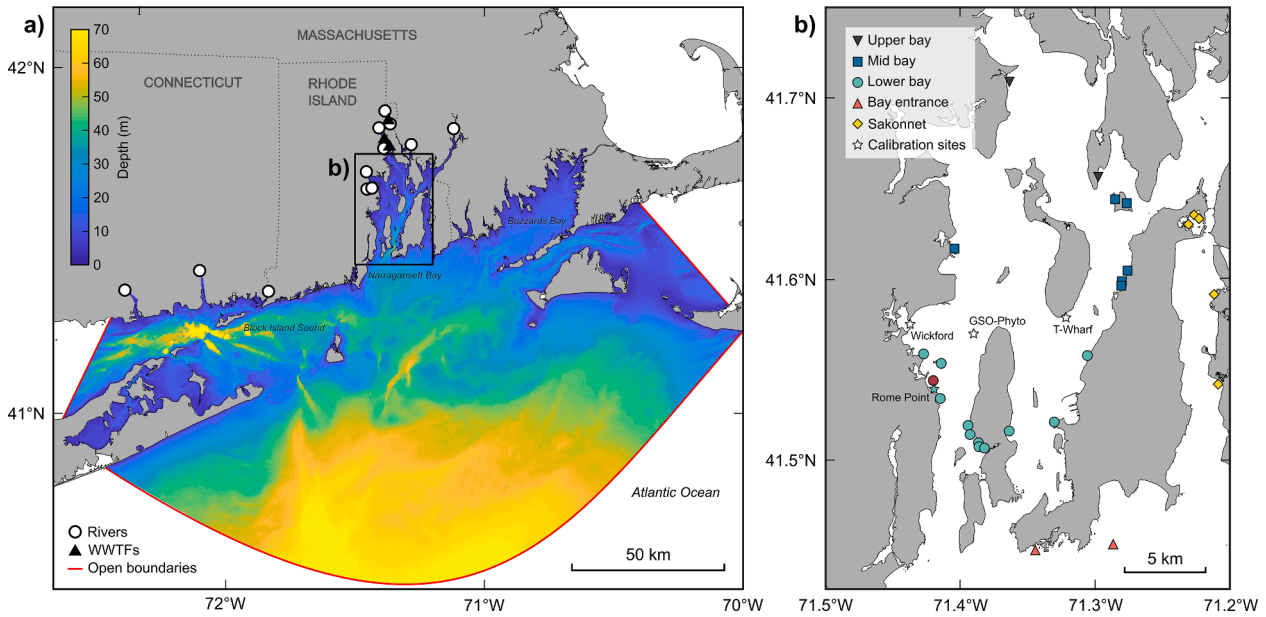
Fig. 1. Map presenting (a) the ecosystem model domain and (b) the location of study sites at existing oyster farms in the Narragansett Bay considered as potential sites for integrated kelp-oyster aquaculture. WWTFs stand for Waste-Water Treatment Facilities. Oyster shell height data collected at the Wickford and Rome Point farms were used to calibrate the oyster bioenergetics (Dynamic Energy Budget; DEB) model.
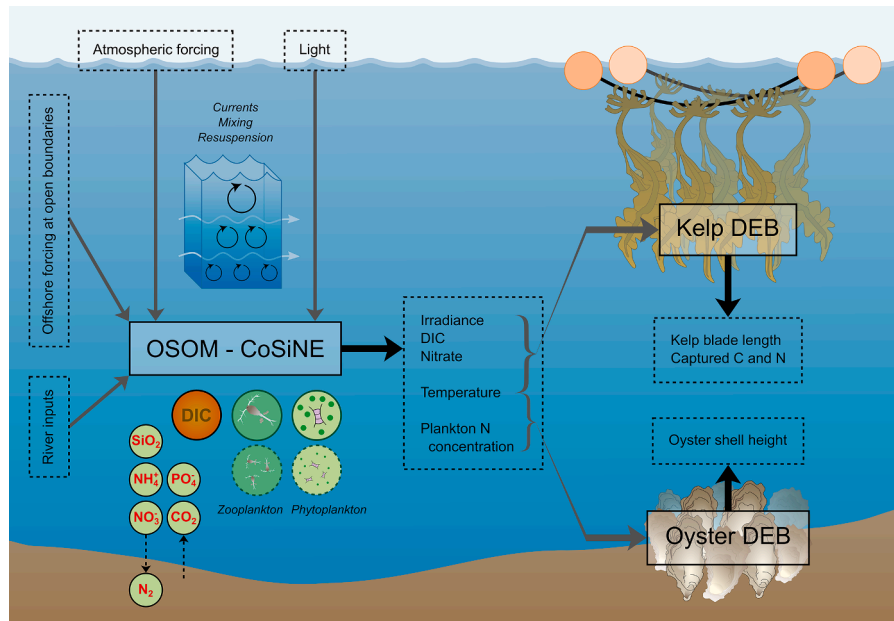

Fig. 2. Conceptual scheme of the ecosystem model for kelp-oyster aquaculture. The hydrodynamic-water quality (OSOM-CoSiNE) model provides forcing variables to the individual kelp and oyster bioenergetics (Dynamic Energy Budget; DEB) models.

vertical and horizontal viscosity and diffusivity, bottom drag, open boundaries forcing, and tidal forcing are described in detail by Sane et al. (2020).

The model was forced with spatially and temporally variable winds from the North American Mesoscale analyses (https://www.ncei.noaa. gov/data/north-american-mesoscale-model/access/historical/analysis). Surface heat fluxes, except for upward longwave radiative flux, which was computed from the model surface temperature, were assumed to be spatially uniform (but still temporally variable). Net shortwave flux and downward longwave fluxes were obtained from the North American Regional Reanalysis model (http://www.emc.ncep.noaa.gov/mm b/rreanl) at the grid point located in the ocean just south of the NB

mouth. Meteorological variables needed to compute sensible and latent heat fluxes were obtained from local PORTS stations (http://www. co-ops.nos.noaa.gov) and from T.F. Green Airport (located along upper NB) and these fluxes as well as surface momentum fluxes were computed using the COARE bulk formulae (Fairall et al., 2003).

Freshwater volume fluxes into the OSOM model domain from rivers and wastewater treatment facilities were applied as point sources at the locations shown in Fig. 1b. For most rivers, measured fluxes were obtained from United States Geological Survey (USGS) gaging stations, and these values were adjusted to account for the ungauged drainage area between the gaging stations and the model input locations (Ullman et al., 2019). The discharge of ungauged rivers was estimated from

nearby gauged rivers using regression techniques as described in Ullman et al. (2019). The salinity of inflowing river water was set to zero while the daily water temperature was specified using an empirical regression using air temperature and water temperature from the prior day (Ullman et al., 2019). Nutrient concentrations in river water were specified using linear interpolation of observations from the Narragansett Bay Commission and the U.S. Geological Survey. Volume fluxes as well as nutrient concentrations for the discharges from the three main wastewater treatment facilities into NB were obtained from the plant operators.

The lower trophic level pelagic ecology of NB was simulated using the Carbon Silicate and Nitrogen Ecosystem (CoSiNE) model (Chai et al., 2002; Xiu and Chai, 2011; Zhou et al., 2017; Liu et al., 2018). CoSiNE is fully coupled with the realistically forced OSOM hydrodynamics model. The model state variables include four nutrients (nitrate, ammonium, phosphate, and silicate), two phytoplankton classes (small phytoplankton and diatoms), two zooplankton classes (micro- and meso-zooplankton), two detritus classes (nitrogenous and silicious detritus), as well as dissolved oxygen, total inorganic carbon, and total alkalinity. Details of the model formulations are described in Chai et al. (2002) and Liu et al. (2018). Nutrient regeneration in the CoSiNE model involves water-column processes only. Because inputs from riverine and wastewater treatment facilities dominate nutrient dynamics in this system (Nixon et al., 1995), benthic regeneration processes can be neglected. The sum of the biomasses of small phytoplankton, diatoms, microzooplankton, and nitrogenous detritus (mmol N m^{-3}) was used as the "food" input in the oyster DEB model.

The coupled OSOM-CoSiNE model was run with a time step of 15 s. Model results were output at 0.5 h intervals and were averaged to the hourly or daily values needed for the kelp or oyster models respectively.

2.4. Kelp and oyster DEB models

The individual bioenergetic models used for kelp and oyster are based on Dynamic Energy Budget (DEB) theory (Kooijman, 2010). Although applied to extremely different organisms, the DEB models for kelp and oyster rely on the same basic principles. Energy contained in a substrate, in the form of DIC and nitrate for kelp or the summed "food" variable described above for oysters, is assimilated into reserves (one for each substrate). Reserves are then used to fuel metabolic processes such as maintenance, somatic growth, development, and reproduction. All parameters and equations for these models are available in Tables S1 and S2.

The kelp DEB model was developed and calibrated by Venolia et al. (2020) and the same set of parameters and initial conditions were used. The model was run on an hourly time step from 1st November 2017 to 23rd April 2018 (i.e., the winter period), which represents a standard growth season for kelp aquaculture in the area, at the end of which algae are harvested and new seed lines deployed the next fall. The kelp blade growth was modelled for an individual grown 1 m underwater at all selected farm site across NB (Fig. 1). Simulations started with a seedling of 50 mg with initial state variables for Nitrogen reserve (m_{EN}) and Carbon reserve (m_{EC}) set at 2 mmol molV^{-1} (i.e., moles of carbon per mole of structure V) and 10 mmol molV^{-1}, respectively. PAR was estimated based on the method described by Venolia et al. (2020), using the same shortwave radiation forcing as was used for the OSOM-CoSiNE model runs. At each location we calculated the expected wet biomass (in kg$_{WW}$ m^{-1}) that could be harvested on a 1-ha farm using weight outputs from the model (in g$_{DW}$ ind^{-1}), a seeding density of 87 ind m^{-1} (mean of 24 samples collected in May 2019, standard deviation: 32; Table S5), and a dry weight to wet weight ratio of 0.10 (mean of 34 samples collected in April 2018, standard deviation: 0.03) for a farm equipped with 100-m lines spaced by 1.5 or 6 m (as experimented on southern New England farms by Yarish et al., 2017).

The oyster DEB model was developed and validated by Lavaud et al. (2017). The same set of parameters was used except for the functional response to food availability (X_K), which was calibrated for this study based on field growth data from two oyster farms (Wickford and Rome Point, Fig. 1b) in lower Narragansett Bay and chlorophyll-*a* concentration measurements obtained from the nearby University of Rhode Island Graduate School of Oceanography's long-term phytoplankton sampling site (station "GSO-phyto" in Fig. 1b). Near-surface and near-bottom chlorophyll-*a* at this site was obtained from seawater samples processed for immediate extraction and quantified by fluorometry as described by Graff and Rynearson (2011). The model was run at the same locations as the kelp model on a daily time step from 1st May 2017 to 31st December 2018 (oysters are usually harvested in their second year of growth). Simulations of oyster shell growth were initiated uniformly across locations with a shell height of 1 cm, half of the maximum reserve density ($E_m = \{\dot{p}_{Am}\}/\dot{v}$) and an empty reproduction buffer. The OSOM-CoSiNE model outputs for the sum of small phytoplankton, diatoms, microzooplankton, and detritus expressed in mmol N m^{-3} was transformed into chlorophyll-*a* concentration assuming a conversion coefficient of unity (Marra et al., 1990; Dugdale et al., 2012) and used as food source in the oyster DEB model. All parameters and equations for these models are available in Tables S3 and S4.

2.5. Revenue analysis of farm-scale operations

Potential biomass was then converted to a monetary value using an average farm-gate price of \$1.32 kg^{-1} or \$0.60 lb^{-1} (fresh) for farmed seaweed in Maine, which is the most recent average price available at the time of writing (Maine Department of Marine Resources, 2020; McKinley Research Group, 2021). Predicted revenue (PR, reported in \$ ha^{-1}) was calculated as: *PR = biomass × density × line length × space × price*, where *biomass* is the DEB model derived individual biomass at harvest (kg$_{WW}$ ind^{-1}), *density* is the seeding density (ind m^{-1}; see 2.3), *line length* is the length of a seeding line (100 m), *space* is the space between lines (1.5 or 6 m; as experimented on southern New England farms by Yarish et al., 2017), and *price* is the average farm-gate price.

Market size for oysters is 3 in (7.4 cm) and they usually reach this threshold during their second year in Connecticut (U.S.). However, the U.S. oyster market is generally based on unit prices independent of oyster size. Since the present model does not represent a population but a generalized individual, we did not calculate the value of produced oysters in this study.

2.6. Ecosystem services

Kelp uses some elements present in the water such as nitrogen (taken up by the algae as NO$_3^-$, NO$_2^-$, or NH$_4^+$) and carbon dioxide to grow. The removal of N and C contributes to the mitigation of nutrient runoff and carbon emissions and as such constitutes ecosystem services that can be quantified through the bioenergetic DEB model. Potential N and C net uptake (kg N/C ha^{-1}) from kelp was output from the DEB model at each location for an average individual and scaled up to a farm setting using the equation: *Uptake = W × density × line length × space*, where *W* is the mass of total N or C in an individual algal thallus (kg ind^{-1}). Because the contribution of reserves in C and N to *W* may vary through time, we report the value of N and C net uptake both at the time of harvest, i.e., at the end of the simulation, as well as the maximum through time. This distinction may indicate that harvest should occur earlier to maximize the nutrient removal service provided by kelp growth.

3. Results

3.1. OSOM-CoSiNE model outputs

The temporal dynamics of environmental variables outputted from the OSOM-CoSiNE model followed a seasonal pattern, more pronounced at the sub-surface where kelp is grown, than near-bottom where most oysters grow (Figs. 3-4). Near-surface temperature reached a minimum
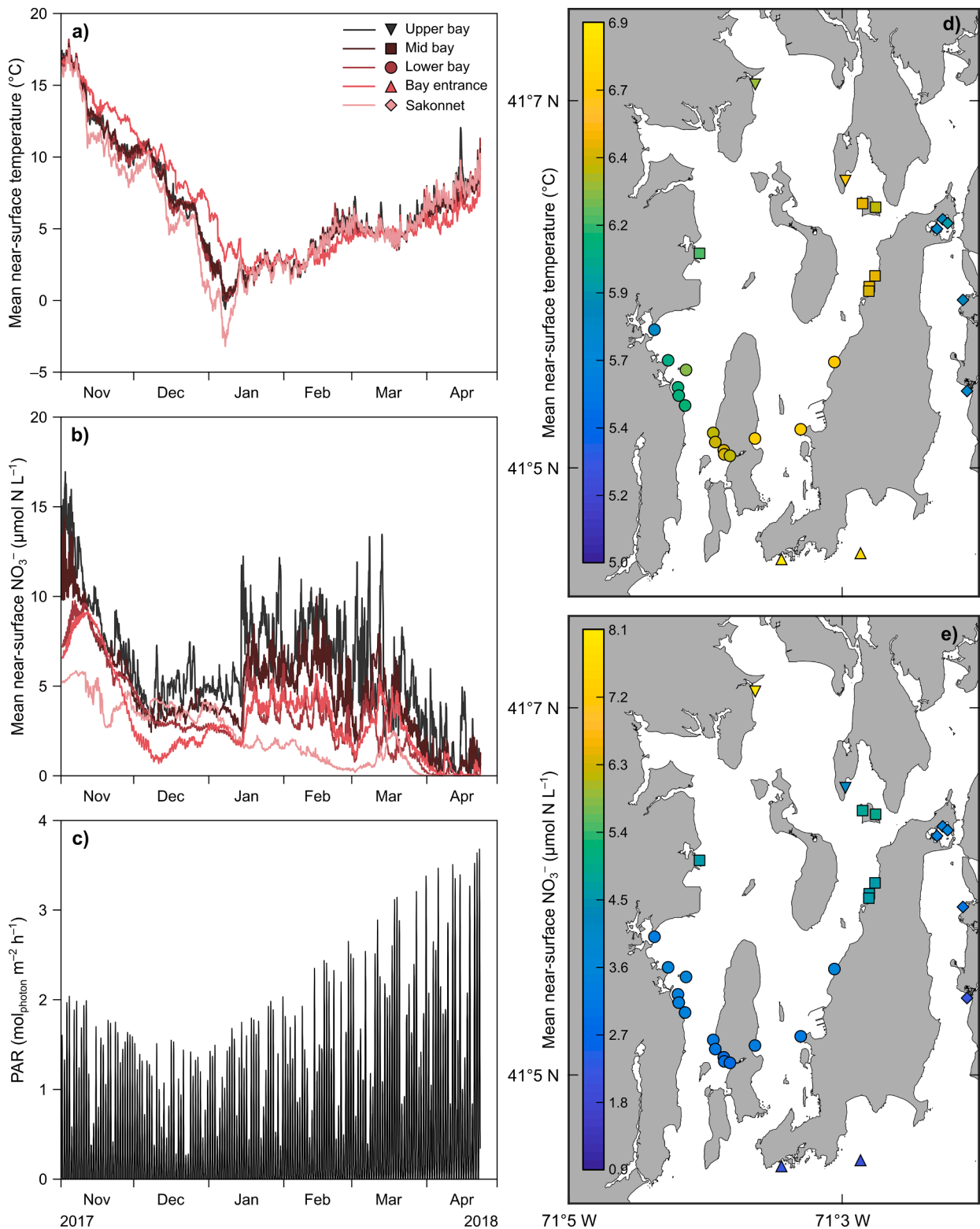
Fig. 3. Mean near-surface temperature (°C; a, d), near-surface nitrate concentration (μmol N L^{-1}; b, e) computed by the ROMS-CoSiNE model and PAR (mol$_{photon}$ m^{-2} h^{-1}; c) between 01 November 2017 and 23 April 2018 by region (graphs on the left) and through time at the selected oyster farms in Narragansett Bay (maps on the right). These forcing variables were used in the kelp DEB model. The same PAR data were used at each site.

in early January before slowly rising again (Fig. 3a). Near-bottom temperatures were also lowest in early January and reached a maximum in early August (Fig. 4a). Near-surface nitrate concentration was highest in early November (maximum values within regions ranging between 5.9 and 16.4 μmol N L^{-1}) and lowest in April (minimum values

<1 μmol N L^{-1} at all sites) with values between 2 and 11 μmol N L^{-1} also observed in all sites except at the Bay Entrance in January–March (Fig. 3b). Near-bottom oyster food concentration showed high variability with peaks throughout the end of spring and the summer with maximum values up to 12 to 16 μmol N L^{-1} (Fig. 4b). PAR, which is not
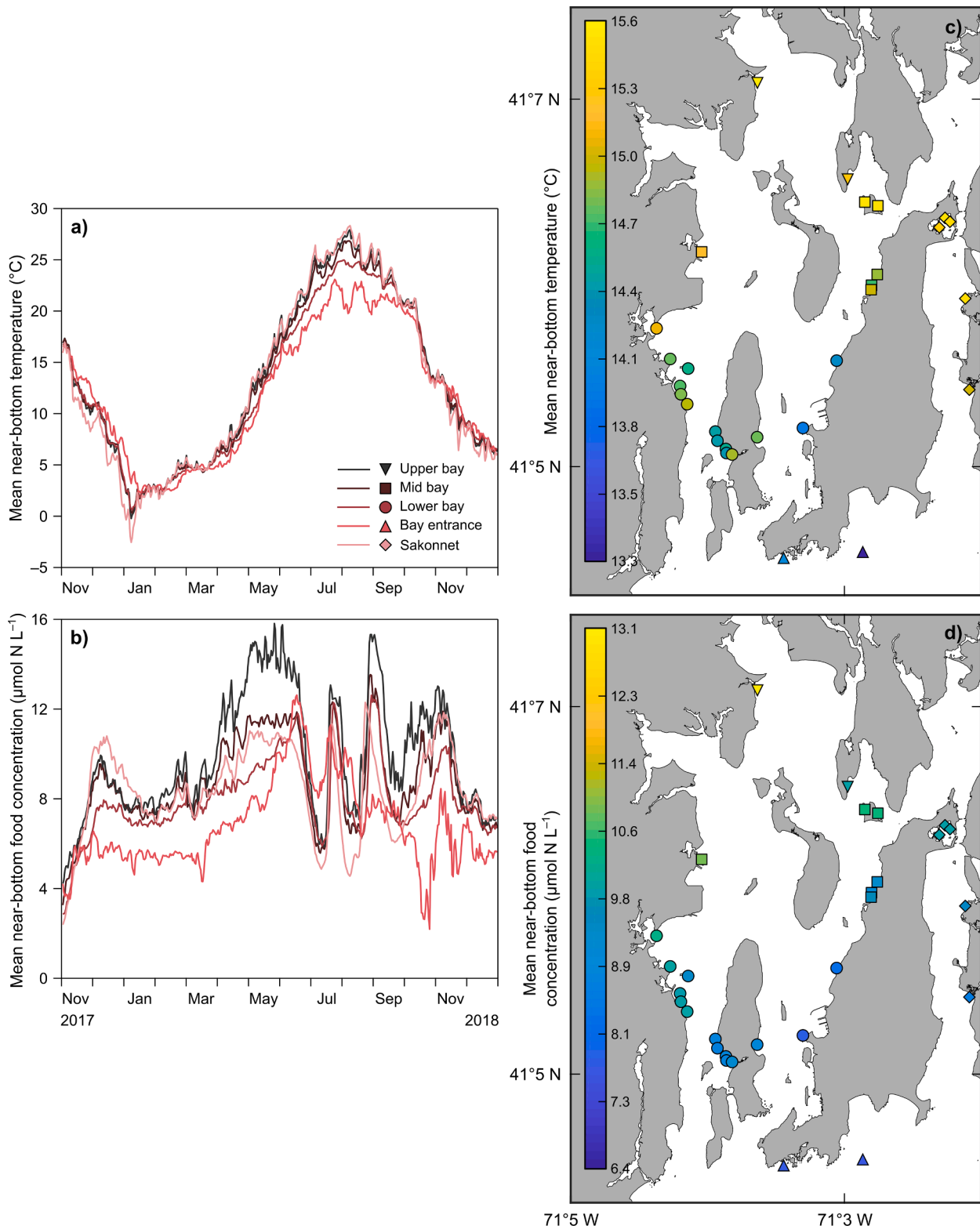
Fig. 4. Mean near-bottom temperature (°C; a, c) and near-bottom oyster food concentration (μmol N L^{-1}; b, d) between 01 May 2017 and 31 December 2018 by region (graphs on the left) and through time at the selected oyster farms in Narragansett Bay (maps on the right). These forcing variables were used in the oyster DEB model. Food is computed as the sum of small phytoplankton, diatoms, microzooplankton, and nitrogenous detritus.

an output from the model, also varied according to the time of the year with minimum average values in December and maximum values at the end of the study period in April (Fig. 3c).

Outputs from OSOM-CoSiNE model were used to force the kelp and oyster models over different time periods: for 6 months (Nov. 2017–Apr.

2018) for kelp and for 20 months (May 2017–Dec. 2018) for oysters. To illustrate the spatial variability of forcing variables for each model (near-surface temperature and nitrate for kelp, and near-bottom temperature and food concentration for oysters), the mean values of the OSOM-CoSiNE output variables were computed over the different model time

periods. For kelp growing mostly during winter months, near-surface temperatures were coldest at the shallow sites along the western side of the bay and in the Sakonnet River and highest in the deeper areas of the Mid and Lower Bay (Fig. 3d). Mean near-surface nitrate concentrations were highest in the Upper Bay (>7.5 µmol N L^{-1}) and lowest at the Bay Entrance (2.2 ± 0.1 µmol N L^{-1}; Fig. 3e). During the nearly 2-year oyster period, mean near-bottom temperatures were highest (>15 °C) in the Upper Bay and in the shallow areas in the western Mid Bay and the Sakonnet River and lowest in the eastern Lower Bay and at the Bay Entrance (Fig. 4c). Mean near-bottom oyster food concentration exhibited a similar north-south gradient, with higher values in the Upper Bay and decreasing southward (Fig. 4d).

3.2. Kelp and oyster growth potential

Mean predicted kelp blade length at the end of the cultivation period in April varied from 50 ± 1 cm at Bay Entrance sites to 74 ± 5 cm at the Upper Bay sites (Fig. 5a). Final mean predicted length at the Sakonnet sites (62 ± 3 cm) was between that of the Lower Bay (58 ± 1 cm) and Mid Bay sites (73 ± 2 cm; overlapping with Upper Bay site in Fig. 5a). Predicted kelp growth slowed greatly in the last month at sites near the entrance of NB, while moderate to high growth rates were still simulated in other parts of the bay. Model predictions of kelp mass ranged from 0.97 kg$_{WW}$ m^{-1} at the easternmost site of Bay Entrance to 2.03 kg$_{WW}$ m^{-1} at the northernmost site in Upper Bay, or 1.6 tons ha^{-1} and 3.4 tons ha^{-1} on 6 m spaced line-farms, respectively (Figure 6a; 6.5 tons ha^{-1} and 13.5 tons ha^{-1} with 1.5 m spaced line-farms). The averages for the entire bay amount to 1.45 ± 0.05 kg$_{WW}$ m^{-1} or 9.6 ± 0.3 tons ha^{-1} (2.4 ± 0.1 tons ha^{-1} with 1.5 m spaced line-farms).

Mean predicted oyster height at the end of the cultivation period in November varied from 6.5 ± 0.3 cm in sites at the Bay Entrance to 7.8 ± 0.3 cm in the Upper Bay sites (Figs. 5b, 6b). As for kelp simulations, predicted growth of oysters in Sakonnet sites (7.4 ± 0.0 cm) was between that of oysters growing in Lower Bay (7.1 ± 0.1 cm) and Mid Bay sites (7.5 ± 0.1 cm; Figs. 5b, 6b). Because this study focuses on the integration of kelp production to existing oyster farms, simulations for oysters ended during their second year of growth. Extrapolation of simulations assuming a repetition of environmental conditions from 2018 in 2019 indicate that all oysters except those at the Bay Entrance sites easily reach market size in their third year of growth (data not shown).

3.3. Production value potential

Average minimum of 6.7 ± 0.3 tons ha^{-1} at Bay Entrance farms, average maximum of 12 ± 1.4 tons ha^{-1} at Upper Bay sites (Table 1). These estimated yields at the Bay Entrance and in the Upper Bay would translate to $2222 and $3998 for 6 m spaced line-farms and to $8887 and $15,991 for 1.5 m spaced line-farms, respectively. Maximum revenue at one site in Upper Bay was estimated at $17,872 for a 1.5 m spaced line-farm while the minimum estimate at the Bay Entrance was $2138 for a 6 m spaced line-farm.

3.4. Ecosystem services

A gradient in N uptake from kelp was predicted by the model from the Bay Entrance to the Upper Bay locations with values ranging from 10 ± 0 kg N ha^{-1} at harvest time in a 6 m spaced line-farm from the Bay Entrance to 1117 ± 332 kg N ha^{-1} at maximum in a 1.5 m spaced line-farm from the Upper Bay (Table 2). The difference between values at harvest time and at maximum reflect the decrease in N reserves observed toward the end of simulations (Fig. 7). Predicted C uptake from kelp through photosynthesis ranged from 1185 ± 161 kg C ha^{-1} in a 6 m spaced line-farm from the Mid Bay region to 6184 ± 157 kg C ha^{-1} in a 1.5 m spaced line-farm from the Lower Bay (Table 2).

4. Discussion

Model simulations indicated that both farmed kelp and oysters should grow well across wide swaths of NB, although not as well as some nearby observations, and that the timing for harvest is critical for maximized growth. Predicted kelp blade length ranged between 50 and 74 cm and biomass between 0.97 and 2.03 kg$_{WW}$ m^{-1} over the cultivation season, which stands at the lower range of observations of 0.2 to 7.8 kg m^{-1} (Table S5). Yarish et al. (2017) also obtained higher yields in a pilot study in Long Island Sound and Southeastern New England (1.6 to 14.8 kg m^{-1}). These authors report, however, that growth was limited in their Rhode Island and Massachusetts sites. At the time of harvest in our study, apical frond loss can become common in NB, which has been correlated with temperature stress and wave action (Krumhansl et al., 2014), mechanical stress of biofouling (Brown et al., 1997), and overall blade length (Sjotun, 1993). Additionally, the limit on growth could be a result of a reduction in N reserves toward the end of the season (see Figure S4a), in link with a decrease in N concentration in the water
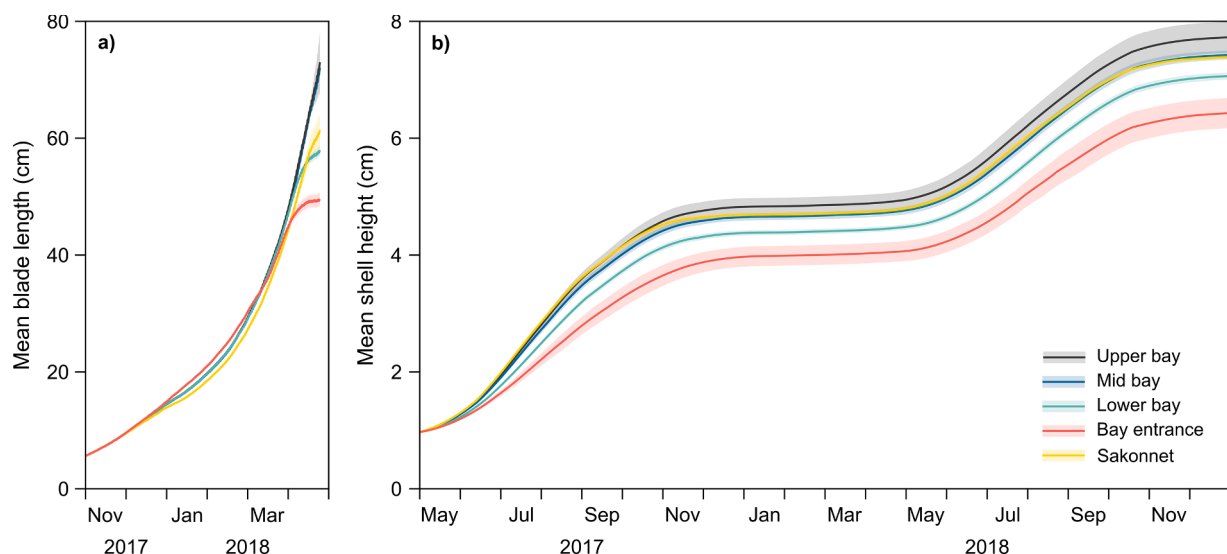

Fig. 5. Predicted mean kelp blade length (a) and oyster shell height (b) at existing oyster farms in Narragansett Bay. The area around the curves represents the standard error of the mean of predictions from farms grouped by location in the bay.
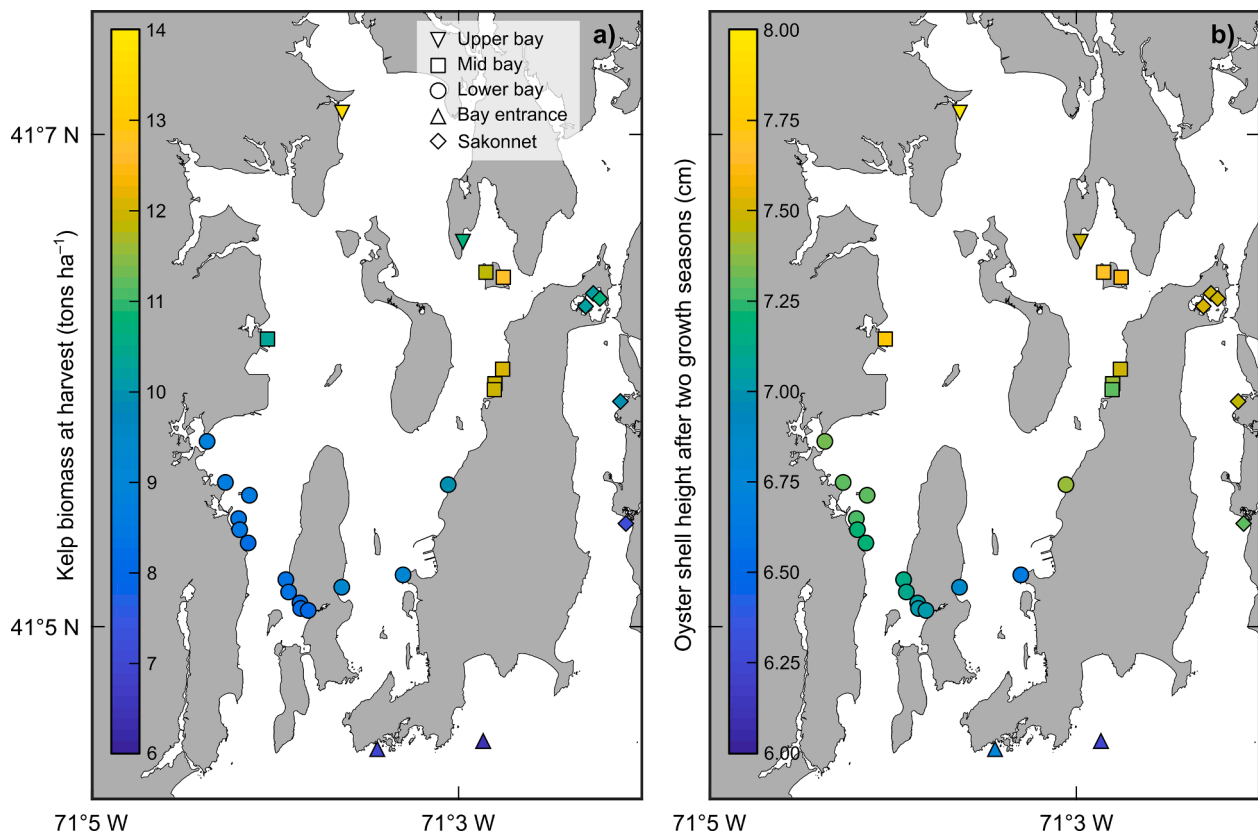
Fig. 6. Spatially explicit predictions of mean kelp biomass per hectare (tons ha^{-1}) at harvest (a) and oyster shell height (cm) after two growth seasons (b) at existing oyster farms in Narragansett Bay. Kelp potential production is presented for a 1.5 m spaced line-farm; the color scale for a 6 m spaced line-farm would vary between 1.5 and 3.5 tons ha^{-1}.

Table 1
Biomass and farm-gate value (USD) estimates of kelp grown on a 1-ha farm with 100-m lines spaced by 1.5 or 6 m.

Location	Biomass (kg m^{-1})	Biomass (kg ha^{-1})		Value ($ ha^{-1})	
		1.5 m	6 m	1.5 m	6 m
Upper Bay	1.82 ± 0.21	12,115 ± 1425	3029 ± 356	15,991 ± 1881	3998 ± 470
Mid Bay	1.77 ± 0.11	11,821 ± 754	2955 ± 189	15,603 ± 995	3901 ± 249
Lower Bay	1.29 ± 0.08	8613 ± 561	2153 ± 140	11,369 ± 741	2842 ± 185
Sakonnet	1.45 ± 0.18	9657 ± 1211	2414 ± 303	12,747 ± 1599	3187 ± 400
Bay Entrance	1.01 ± 0.04	6733 ± 253	1683 ± 63	8887 ± 334	2222 ± 84
Average	1.45 ± 0.27	9639 ± 1816	2410 ± 454	12,724 ± 2397	3181 ± 599

Table 2
Nitrogen (N) and Carbon (C) fixation by kelp grown on a 1-ha farm with 100-m lines spaced by 1.5 or 6 m at the time of harvest, at time of maximum weight, and cumulated over a growing season (173 days).

Location	Time	Fixed Nitrogen (kg N ha^{-1})		Fixed Carbon (kg C ha^{-1})	
		1.5 m	6 m	1.5 m	6 m
Upper Bay	harvest	635 ± 545	159 ± 136	4766 ± 1961	1192 ± 490
	at maximum	1117 ± 332	279 ± 83	4766 ± 1961	1192 ± 490
Mid Bay	harvest	258 ± 61	65 ± 15	4741 ± 644	1185 ± 161
	at maximum	945 ± 58	236 ± 15	4741 ± 644	1185 ± 161
Lower Bay	harvest	63 ± 19	16 ± 5	6184 ± 157	1546 ± 39
	at maximum	563 ± 79	141 ± 20	6184 ± 157	1546 ± 39
Sakonnet	harvest	117 ± 39	29 ± 10	5977 ± 294	1494 ± 74
	at maximum	663 ± 183	166 ± 46	5977 ± 294	1494 ± 74
Bay Entrance	harvest	39 ± 2	10 ± 0	5134 ± 183	1283 ± 46
	at maximum	245 ± 19	61 ± 5	5134 ± 183	1283 ± 46

(Fig. 3b), indicating an N shortage for growth. While increases in light flux and temperature in the spring favor C assimilation in kelps, the basic somatic maintenance costs are also expected to increase (Figure S4b). But with a limited supply of N, the growth rate of algae starts to decrease.

Another factor potentially affecting our kelp growth estimates is competition with microalgae in Upper Bay sites. As the coupling of the ROMS-CoSiNE model to the kelp and oyster DEB models was operated offline, no feedback interaction from kelps or oysters on the 3D model occurred. The filtration activity of oysters feeding on phytoplankton and the competition for light and nutrients between macro- and microalgae could positively influence the actual availability of essential substrates for kelp growth. The lower kelp biomass predicted by the model

compared to available data could also be due to the average seeding density of 87 ind m^{-1} used in our calculations, which is lower than values reported in a case study in Norway by Forbord et al. (2020). It is very likely that not all seeded kelp develops into fully grown thalli, especially at high densities. Yarish et al. (2017) reported farm-scale biomass production values of 1.0 tons ha^{-1} on 6 m spaced line-farms
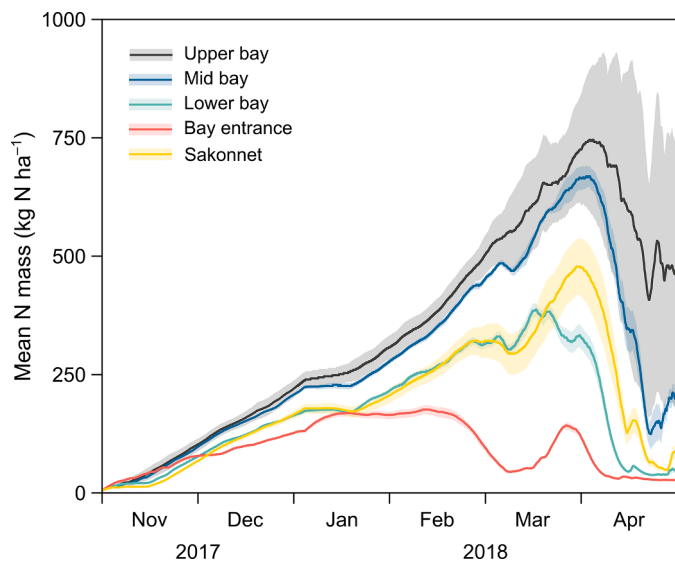
Fig. 7. Predicted mean N mass from kelp tissue at existing oyster farms in Narragansett Bay. The area around the curves represents the standard error of the mean of predictions from farms grouped by location.

and 4.4 tons ha^{-1} on 1.5 m spaced line-farms which is within our estimates that ranged between 1.7 ± 0.1 and 12 ± 1.4 tons ha^{-1}. Note that the different line spacing scenarios used in our simulations represent a simple scale up of individual dynamics and not different model runs. Moreover, the depth at which the growing lines are set is another factor that can impact kelp harvest biomass through light availability. We assumed that algae were grown at a depth of 1 m at all growing sites, like Forbord et al. (2020) who used depth of 1 to 2 m, while Yarish et al. (2017) did not specify this information.

As for many organisms, inter-individual variability in physiological traits can be important, and accounting for this pattern could lead to more accurate predictions and remove the need for rule-of-thumb estimates (Koch and De Schamphelaere, 2020). We started simulations with uniform oyster height across stations/sites (1 cm), which does not account for the environmental history that individual oysters would have experienced while growing at these different locations since their deployment (usually around 3–4 mm). This starting size was based on data collected for the calibration of the half-saturation coefficient (Figure S3), but more variation should be expected. Additionally, different oyster culture practices (e.g., line, raft) would also likely influence growth compared to traditional on-bottom culture (modeled in this study), with possible impacts on light availability and nutrient circulation and availability for kelp (Strohmeier et al., 2005)

The highest growth rates for farmed kelp and oysters were predicted in the Upper Bay sites, where both organisms benefited from higher concentrations of nitrate and near-bottom concentrations of phytoplankton, respectively. The elevated nitrate concentration predicted in this area, which is consistent with observations (e.g., Oviatt et al., 2017), is due to the location of three large wastewater treatment facilities and two of the largest tributary rivers at the northern end of the Bay (Fig. 1). Freshwater runoff could, however, pose a limit to growth because sugar kelps prefer high salinity waters, particularly at lower latitudes (Monteiro et al., 2021). Salinity is not currently included in the kelp DEB model but could be added as a forcing variable as has been done for other organisms living in environments subjected to high salinity variations (Lavaud et al., 2017).

Oyster farms located at the Bay Entrance appear to be the least suited for kelp cultivation as suggested by the smaller simulated blade lengths (Fig. 5a). Lower phytoplankton concentration in more open waters has been used to explain reduced growth rates in bivalves in studies on offshore aquaculture (Palmer et al., 2021). Farms located further south

of NB would also involve higher operation costs due to the distance to site and the exposure to wave action potentially involving heavier gear to secure lines. With production potential yielding about half of the value expected at Upper Bay locations (Table 2), the development of kelp aquaculture at the entrance of NB might be limited, according to model outputs, although kelp has been successfully grown along southern New England shorelines, including Connecticut and Massachusetts (Kim et al., 2019; Heidkamp et al., 2022). One factor that may compensate lower growth is the density of farm lines which previous studies suggested could provide high yield in tightly spaced (1.5 m) lines (Yarish et al., 2017; Umanzor et al., 2021). However, most experimental studies conducted on existing farms generally adopt wider separation (about 5–6 m) between lines (e.g., Tabassum et al., 2017; Grebe et al., 2021) and feedback from farmers is needed to evaluate the practicality of working and maintaining such a design in a more exposed environment such as the NB Entrance.

Our ecosystem model demonstrates significant quantities of N are removed from the system via kelp growth (Table 2). However, the bio-extraction capacity (estimated between 10 and 1117 kg N ha^{-1}) showed high variability depending on the location in NB and line spacing. The estimated range encompasses values of 19 to 176 kg N ha^{-1} calculated by Grebe et al. (2021) in a recent study on kelp aquaculture potential in Maine and those of 10 to 139 kg N ha^{-1} obtained by Kim et al. (2015). As for biomass production, which N uptake is directly linked to, various assumptions regarding farm characteristics may explain the higher range of N removed by kelp in our study, including line spacing, initial seeding density, duration of growing season, and harvest date. As shown in Table 2, maximum blade length does not necessarily mean maximum N removal (through harvest) as N availability tends to decrease later in the growing season, with more uptake from both macro- and micro-algae due to higher biomass and a reduction in runoff. The predicted drop in N content in kelp tissue at the end of the simulated period may be surprising considering the capacity of sugar kelp to store nitrogen (Stekoll et al., 2021). However, other studies also showed reductions in N content in kelp tissues particularly at the end of the growth season (Kim et al., 2015; Stekoll et al., 2021). More data on the temporal dynamics of N in kelp tissue could be used to refine model parameters related to the mobilization of N reserves and the needs for structural N maintenance.

The development of macroalgae cultivation is also seen as a mitigation tool for C emissions from land-based activities (Doumeizel et al., 2020; Park et al., 2021), although these impacts are limited when macroalgae are harvested vs. buried in the deep ocean (Dolliver and O'Connor, 2022). Similarly, it should be possible to evaluate the C removal potential from oysters through biocalcification. This can be achieved within the DEB framework as bio-calcified products can be computed as a weighted sum of mineral fluxes resulting from metabolic processes (see Pecquerie et al., 2012, or Galli et al., 2016, for examples of biocalcification in DEB). The current model for *S. latissima* still requires upgrades to account for dark respiration and produce net estimates of C uptake (Venolia et al., 2020), but the structure of the model could be transferred to any macroalgal or microalgal species.

With the offline coupling of the hydrodynamic model to bioenergetic models for kelp and oysters, the present work constitutes a first step in evaluating the production potential for integrated aquaculture in NB. Further developments including the budgeting of nutrients within the system would allow the quantification of N fluxes using the current modeling approach. Such an analysis based on individual DEB models was recently undertaken in Eastern Canada to evaluate the relationship between opportunistic macroalgae growth, mussel aquaculture, and natural bivalve species (Lavaud et al., 2021) and could be applied in future studies in NB. As kelp competes for nutrients with phytoplankton, which constitute the main food source of oysters, the indirect effect of kelp on oysters could be assessed to maximize production efficiency. Nevertheless, such impacts are likely minimal because: 1) optimal growth periods for kelp and phytoplankton are temporally decoupled

(until mid-late spring), and 2) the scale of kelp deployment in existing farms is relatively small compared to the rest of the bay. Our model could also be used in forecasting mode to mechanistically predict the system production potential based on future climate predictions (Jiang et al., 2022).

Our ecosystem model simulations provide estimates of the growth potential for kelp at existing eastern oyster farms across NB. Results demonstrate there are potentially significant ecological and economic benefits of such operations. These predictions offer a promising outlook and should help producers and managers in their decision-making process for this relatively new industry in the U.S. Following assumptions from Yarish et al. (2017) who conducted an analysis of the kelp production industry in northeastern U.S., we showed that kelp farming in NB would generate economically sustainable yields in the upper and middle sections of the bay. Combined with existing oyster farming operations, several operational costs would likely be reduced due to similar technologies being used: gear and operation tools like boats, mooring, processing facilities would be used for both species. Varying yields due to forcing parameters controlling kelp growth (N load, temperature, PAR) would likely have an impact on handling time at harvest and during processing, which is hard to quantify at this stage without additional work on economic and environmental condition scenarios. We have described how the time of harvest impacted the bio-extraction capacity of N from the system. The timing of harvest would also have important economic effects because as the season progresses and seawater warms up, apical frond loss increases (Sjøtun, 1993; Krumhansl et al., 2014). Using real-time monitoring of environmental conditions at a particular site would allow precise determination of when harvest should occur. This capacity and the availability of data has been greatly increased in recent years with the deployment of monitoring stations through federal or state programs. Finally, the farming of another product grown on the same aquaculture lease can constitute a means of diversification, with the added benefit of decoupled growth through time (oysters primarily grow during summer months while kelp grows and is farmed only during winter months). The present study provides quantitative estimates of the potential for integrated kelp and oyster aquaculture that will be useful for the development of this type of industry.

CRediT authorship contribution statement

Romain Lavaud: Conceptualization, Methodology, Software, Formal analysis, Investigation, Writing – original draft, Writing – review & editing, Visualization. **David S. Ullman:** Methodology, Software, Investigation, Writing – review & editing, Visualization. **Celeste Venolia:** Methodology, Software, Formal analysis, Writing – review & editing. **Carol Thornber:** Investigation, Writing – review & editing, Funding acquisition. **Lindsay Green-Gavrielidis:** Investigation, Writing – review & editing, Funding acquisition. **Austin Humphries:** Conceptualization, Methodology, Investigation, Resources, Writing – original draft, Writing – review & editing, Supervision, Project administration, Funding acquisition.

Declaration of Competing Interest

The authors declare that they have no known competing financial interests or personal relationships that could have appeared to influence the work reported in this paper.

Data availability

Data will be made available on request.

Supplementary materials

Supplementary material associated with this article can be found, in the online version, at doi:10.1016/j.ecolmodel.2023.110370.

References

Barbier, E.B., Hacker, S.D., Kennedy, C., Koch, E.W., Stier, A.C., Silliman, B.R., 2011. The value of estuarine and coastal ecosystem services. Ecol. Monogr. 81 (2), 169–193.

Barrett, L.T., Theuerkauf, S.J., Rose, J.M., Alleway, H.K., Bricker, S.B., Parker, M., Petrolia, D.R., Jones, R.C., 2022. Sustainable growth of non-fed aquaculture can generate valuable ecosystem benefits. Ecosyst. Serv. 53, 101396.

Bostock, J., McAndrew, B., Richards, R., Jauncey, K., Telfer, T., Lorenzen, K., Little, D., Ross, L., Handisyde, N., Gatward, I., Corner, R., 2010. Aquaculture: global status and trends. Philos. Trans. R. Soc. B: Biol. Sci. 365 (1554), 2897–2912.

Cabral, P., Levrel, H., Viard, F., Frangoudes, K., Girard, S., Scemama, P., 2016. Ecosystem services assessment and compensation costs for installing seaweed farms. Mar. Policy 71, 157–165.

Chai, F., Dugdale, R.C., Peng, T.H., Wilkerson, F.P., Barber, R.T., 2002. One-dimensional ecosystem model of the equatorial Pacific upwelling system. Part I: model development and silicon and nitrogen cycle. Deep Sea Res. Part II 49 (13–14), 2713–2745.

Chopin, T., Yarish, C., Wilkes, R., Belyea, E., Lu, S., Mathieson, A., 1999. Developing Porphyra/salmon integrated aquaculture for bioremediation and diversification of the aquaculture industry. J. Appl. Phycol. 11, 463–484.

Cranford, P.J., Reid, G.K., Robinson, S.M., 2013. Open water integrated multi-trophic aquaculture: constraints on the effectiveness of mussels as an organic extractive component. Aquac. Environ. Interact. 4 (2), 163–173.

Dalton, T.M., Jin, D., 2018. Attitudinal factors and personal characteristics influence support for shellfish aquaculture in Rhode Island (US) coastal waters. Environ. Manage. 61 (5), 848–859.

Dolliver, J., O'Connor, N.E., 2022. Estimating growth, loss and potential carbon sequestration of farmed kelp: a case study of *Saccharina latissima* at Strangford Lough, Northern Ireland. Appl. Phycol. 3 (1), 324–339.

Doumeizel, V., Aass, K., McNevin, A., Cousteau, A., Yap, A.Y., Cai, J., Cottier-Cook, E.J., Giercksky, E., Chen, H., Skjermo, J., 2020. Seaweed Revolution: a Manifesto for a Sustainable Future. Lloyd's Register Foundation, London, UK, pp. 1–16.

Dowd, M., 2005. A bio-physical coastal ecosystem model for assessing environmental effects of marine bivalve aquaculture. Ecol. Modell. 183 (2–3), 323–346.

Dugdale, R., Wilkerson, F., Parker, A.E., Marchi, A., Taberski, K., 2012. River flow and ammonium discharge determine spring phytoplankton blooms in an urbanized estuary. Estuarine Coast. Shelf Sci. 115, 187–199.

European Commission, 2012. Communication from the Commission to the European Parliament, the Council, the European Economic and Social Committee and the Committee of the Regions on Blue Growth Opportunities for Marine and Maritime Sustainable Growth. Publications Office of the European Union, Luxembourg. COM/2012/0494 final.

Fairall, C.W., Bradley, E.F., Hare, J.E., Grachev, A.A., Edson, J.B., 2003. Bulk parameterization of air–sea fluxes: updates and verification for the COARE algorithm. J. Clim. 16 (4), 571–591.

FAO, 2020. The State of World Fisheries and Aquaculture 2020: Sustainability in Action. Food and Agriculture Organization of the United Nations, Rome, p. 224.

Ferreira, J.G., Hawkins, A.J.S., Bricker, S.B., 2007. Management of productivity, environmental effects and profitability of shellfish aquaculture—the Farm Aquaculture Resource Management (FARM) model. Aquaculture 264 (1–4), 160–174.

Froehlich, H.E., Gentry, R.R., Halpern, B.S., 2017. Conservation aquaculture: shifting the narrative and paradigm of aquaculture's role in resource management. Biol. Conserv. 215, 162–168.

Gallardi, D., 2014. Effects of bivalve aquaculture on the environment and their possible mitigation: a review. Fisheries Aquac. J. 5 (3), 1000105.

Galli, G., Bramanti, L., Priori, C., Rossi, S., Santangelo, G., Tsounis, G., Solidoro, C., 2016. Modelling red coral (*Corallium rubrum*) growth in response to temperature and nutrition. Ecol. Modell. 337, 137–148.

Gibbs, M.T., 2009. Implementation barriers to establishing a sustainable coastal aquaculture sector. Mar. Policy 33 (1), 83–89.

Graff, J.R., Rynearson, T.A., 2011. Extraction method influences the recovery of phytoplankton pigments from natural assemblages. Limnol. Oceanogr.: Methods 9, 129–139.

Grant, J., Strand, Ø., 2019. Introduction to provisioning services. Goods and Services of Marine Bivalves. Springer, Cham, pp. 3–5.

Grebe, G.S., Byron, C.J., Brady, D.C., Geisser, A.H., Brennan, K.D., 2021. The nitrogen bioextraction potential of nearshore *Saccharina latissima* cultivation and harvest in the Western Gulf of Maine. J. Appl. Phycol. 33 (3), 1741–1757.

Guyondet, T., Comeau, L.A., Bacher, C., Grant, J., Rosland, R., Sonier, R., Filgueira, R., 2015. Climate change influences carrying capacity in a coastal embayment dedicated to shellfish aquaculture. Estuaries Coasts 38 (5), 1593–1618.

Heidkamp, C.P., Krak, L.V., Kelly, M.M.R., Yarish, C., 2022. Geographical considerations for capturing value in the US sugar kelp (*Saccharina latissima*) industry. Mar. Policy 144, 105221.

Holdt, S.L., Edwards, M.D., 2014. Cost-effective IMTA: a comparison of the production efficiencies of mussels and seaweed. J. Appl. Phycol. 26 (2), 933–945.

Jackson, G.A., Winant, C.D., 1983. Effect of a kelp forest on coastal currents. Cont. Shelf Res. 2 (1), 75–80.

Jiang, L., Blommaert, L., Jansen, H.M., Broch, O.J., Timmermans, K.R., Soetaert, K., 2022. Carrying capacity of *Saccharina latissima* cultivation in a Dutch coastal bay: a modelling assessment. ICES J. Mar. Sci. 79 (3), 709–721.

Kellner, J.B., Sanchirico, J.N., Hastings, A., Mumby, P.J., 2011. Optimizing for multiple species and multiple values: tradeoffs inherent in ecosystem-based fisheries management. Conserv. Lett. 4 (1), 21–30.

Kim, J.K., Kraemer, G.P., Yarish, C., 2015. Use of sugar kelp aquaculture in Long Island Sound and the Bronx River Estuary for nutrient extraction. Mar. Ecol. Prog. Ser. 531, 155–166.

Kim, J., Stekoll, M., Yarish, C., 2019. Opportunities, challenges and future directions of open-water seaweed aquaculture in the United States. Phycologia 58 (5), 446–461.

Knapp, G., Rubino, M.C., 2016. The political economics of marine aquaculture in the United States. Rev. Fisheries Sci. Aquac. 24 (3), 213–229.

Koch, J., De Schamphelaere, K.A., 2020. Estimating inter-individual variability of dynamic energy budget model parameters for the copepod *Nitocra spinipes* from existing life-history data. Ecol. Modell. 431, 109091.

Kooijman, S.A.L.M., 2010. Dynamic Energy Budget Theory for Metabolic Organisation. Cambridge university press, p. 514.

Krumhansl, K.A., Lauzon-Guay, J.S., Scheibling, R.E., 2014. Modeling effects of climate change and phase shifts on detrital production of a kelp bed. Ecology 95 (3), 763–774.

Lavaud, R., La Peyre, M.K., Casas, S.M., Bacher, C., La Peyre, J.F., 2017. Integrating the effects of salinity on the physiology of the eastern oyster, *Crassostrea virginica*, in the northern Gulf of Mexico through a Dynamic Energy Budget model. Ecol. Modell. 363, 221–233.

Lavaud, R., Guyondet, T., Filgueira, R., Tremblay, R., Comeau, L.A., 2020. Modelling bivalve culture-Eutrophication interactions in shallow coastal ecosystems. Mar. Pollut. Bull. 157, 111282.

Liu, Q., Chai, F., Dugdale, R., Chao, Y., Xue, H., Rao, S., Wilkerson, F., Farrara, J., Zhang, H., Wang, Z., Zhang, Y., 2018. San Francisco Bay nutrients and plankton dynamics as simulated by a coupled hydrodynamic-ecosystem model. Cont. Shelf Res. 161, 29–48.

Lotze, H.K., Lenihan, H.S., Bourque, B.J., Bradbury, R.H., Cooke, R.G., Kay, M.C., Kidwell, S.M., Kirby, M.X., Peterson, C.H., Jackson, J.B., 2006. Depletion, degradation, and recovery potential of estuaries and coastal seas. Science 312 (5781), 1806–1809.

Maine Department of Marine Resources, 2020. Marine algae harvest data (2015–2020). Last accessed on 2022/09/23 at: https://www.maine.gov/dmr/aquaculture/maine-aquaculture-leases-and-lpas/maine-aquaculture-leases-and-lpas.

Marra, J., Bidigare, R.R., Dickey, T.D., 1990. Nutrients and mixing, chlorophyll and phytoplankton growth. Deep-Sea Res. 37 (1), 127–143.

Matthewson, J., Weisberg, M., 2009. The structure of tradeoffs in model building. Synthese 170 (1), 169–190.

McKinley Research Group, 2021. Alaska seaweed market assessment. Report prepared for Alaska Fisheries Development Foundation. August 2021. 79 p.

Monteiro, C., Li, H., Diehl, N., Collén, J., Heinrich, S., Bischof, K., Bartsch, I., 2021. Modulation of physiological performance by temperature and salinity in the sugar kelp *Saccharina latissima*. Phycol. Res. 69 (1), 48–57.

Nixon, S.W., Granger, S.L., Nowicki, B.L., 1995. An assessment of the annual mass balance of carbon, nitrogen, and phosphorus in Narragansett Bay. Biogeochemistry 31 (1), 15–61.

NOAA Alaska Fisheries Science Center, 2022. Aquaculture strategic science plan. August 2022. 22 p.

Oviatt, C., Smith, L., Krumholz, J., Coupland, C., Stoffel, H., Keller, A., McManus, M.C., Reed, L., 2017. Managed nutrient reduction impacts on nutrient concentrations, water clarity, primary production, and hypoxia in a north temperate estuary. Estuarine Coast. Shelf Sci. 199, 25–34.

Palmer, S.C., Barillé, L., Kay, S., Ciavatta, S., Buck, B., Gernez, P., 2021. Pacific oyster (*Crassostrea gigas*) growth modelling and indicators for offshore aquaculture in Europe under climate change uncertainty. Aquaculture 532, 736116.

Park, J.S., Shin, S.K., Wu, H., Yarish, C., Yoo, H.I., Kim, J.K., 2021. Evaluation of nutrient bioextraction by seaweed and shellfish aquaculture in Korea. J. World Aquac. Soc. 52 (5), 1118–1134.

Pecquerie, L., Fablet, R., De Pontual, H., Bonhommeau, S., Alunno-Bruscia, M., Petitgas, P., Kooijman, S.A., 2012. Reconstructing individual food and growth histories from biogenic carbonates. Mar. Ecol. Prog. Ser. 447, 151–164.

Sane, A., Fox-Kemper, B., Ullman, D.S., Kincaid, C., Rothstein, L., 2020. Consistent predictability of the Ocean State Ocean Model (OSOM) using information theory and flushing timescales. J. Geophys. Res.: Oceans, e2020JC016875.

Shchepetkin, A.F., McWilliams, J.C., 2005. The regional oceanic modeling system (ROMS): a split-explicit, free-surface, topography-following-coordinate oceanic model. Ocean Modell. 9 (4), 347–404.

Sjøtun, K., 1993. Seasonal lamina growth in two age groups of *Laminaria saccharina* (L.) Lamour. in western Norway. Botanica Marina 36 (5), 433–442.

Smaal, A.C., Ferreira, J.G., Grant, J., Petersen, J.K., Strand, Ø., 2019. Goods and Services of Marine Bivalves. Springer Nature, p. 591.

Smith, B., 2019. Eat like a fish. Knopf 320.

Stankus, A., 2021. Webinar: regional Review on Status and Trends in Aquaculture Development in North America - 2020. FAO Aquac. Newslett. 63, 25–26.

Stekoll, M.S., Peeples, T.N., Raymond, A.E., 2021. Mariculture research of *Macrocystis pyrifera* and *Saccharina latissima* in Southeast Alaska. J. World Aquac. Soc. 52 (5), 1031–1046.

Strohmeier, T., Aure, J., Duinker, A., Castberg, T., Svardal, A., Strand, Ø., 2005. Flow reduction, seston depletion, meat content and distribution of diarrhetic shellfish toxins in a long-line blue mussel (Mytilus edulis) farm. J. Shellfish Res. 24 (1), 15–23.

Tabassum, M.R., Xia, A., Murphy, J.D., 2017. Potential of seaweed as a feedstock for renewable gaseous fuel production in Ireland. Renewable Sustainable Energy Rev. 68, 136–146.

Tallman, J.C., Forrester, G.E., 2007. Oyster grow-out cages function as artificial reefs for temperate fishes. Trans. Am. Fish. Soc. 136 (3), 790–799.

Tang, Q., Zhang, J., Fang, J., 2011. Shellfish and seaweed mariculture increase atmospheric CO_2 absorption by coastal ecosystems. Mar. Ecol. Prog. Ser. 424, 97–104.

Theuerkauf, S.J., Barrett, L.T., Alleway, H.K., Costa-Pierce, B.A., St. Gelais, A., Jones, R. C., 2021. Habitat value of bivalve shellfish and seaweed aquaculture for fish and invertebrates: pathways, synthesis and next steps. Rev. Aquac. 14 (1), 54–72.

Ullman, D.S., Kincaid, C., Balt, C., Codiga, D.L., 2019. Hydrodynamic Modeling of Narragansett Bay in Support of the EcoGEM Ecological Model. Graduate School of Oceanography. University of Rhode Island, Narragansett, RI, p. 58. Technical Report No. 2019-01.

Venolia, C.T., Lavaud, R., Green-Gavrielidis, L.A., Thornber, C., Humphries, A.T., 2020. Modeling the growth of sugar kelp (*Saccharina latissima*) in aquaculture systems using dynamic energy budget theory. Ecol. Modell. 430, 109151.

Worm, B., Barbier, E.B., Beaumont, N., Duffy, J.E., Folke, C., Halpern, B.S., Jackson, J.B., Lotze, H.K., Micheli, F., Palumbi, S.R., Sala, E., 2006. Impacts of biodiversity loss on ocean ecosystem services. Science 314 (5800), 787–790.

Xiu, P., Chai, F., 2011. Modeled biogeochemical responses to mesoscale eddies in the South China Sea. J. Geophys. Res.: Oceans 116 (C10), 006.

Yarish, C., Kim, J.K., Lindell, S., Kite-Powell, H., 2017. Developing an Environmentally and Economically Sustainable Sugar Kelp Aquaculture Industry in Southern New England: from Seed to Market. EEB Articles, p. 38.

Ysebaert, T., Walles, B., Haner, J., Hancock, B., 2019. Habitat modification and coastal protection by ecosystem-engineering reef-building bivalves. Goods and Services of Marine Bivalves. Springer, Cham, pp. 253–273.

Zhou, F., Chai, F., Huang, D., Xue, H., Chen, J., Xiu, P., Xuan, J., Li, J., Zeng, D., Ni, X., Wang, K., 2017. Investigation of hypoxia off the Changjiang Estuary using a coupled model of ROMS-CoSiNE. Prog. Oceanogr. 159, 237–254.